ELSEVIER

Catalysis Today 50 (1999) 553–565

CATALYSIS TODAY

Adsorption and reactions at the (0 1 0) V_2O_5 surface: cluster model studies

M. Witko[a,*], K. Hermann[b], R. Tokarz[a]

[a]*Institute of Catalysis and Surface Chemistry, Polish Academy of Sciences, ul. Niezapominajek, 30 239, Cracow, Poland*
[b]*Fritz-Haber-Institut der Max-Planck-Gesellschaft, Faradayweg 4-6, 14195, Berlin, Germany*

Abstract

The use of quantum chemical approaches in the description of electronic properties of a catalyst and in understanding the mechanism of catalytic reactions is discussed. The electronic structure of vanadium pentoxide, V_2O_5, is studied based upon the cluster model with ab initio DFT and semiempirical INDO-type methods. Inter-atomic binding in vanadium pentoxide is determined to be of a mixed ionic and covalent character. Convergence of the electronic properties with respect to the cluster size is achieved for clusters as large as $V_{10}O_{31}H_{12}$. Similar electronic parameters of the $V_{10}O_{31}H_{12}$ cluster in its idealized, bulk and optimized geometry are obtained. The effect of the second substrate layer on the electronic properties is found to be negligible. The calculations reveal differences in the catalytic properties between structurally inequivalent surface oxygen centers and show the increased local reactivity of bridging oxygens with respect to the electrophilic adparticles. The results of the adsorption of hydrogen, treated as a probe reaction to model the first step in the selective oxidation of hydrocarbons at structurally different oxygen sites, are compared with the adsorption/activation of aliphatic (propene) and aromatic (toluene) hydrocarbons at the vanadium pentoxide(0 1 0) surface. The H/H^+ species adsorbs at the V_2O_5(0 1 0) surface always at oxygen sites forming stable surface hydroxyl groups. The detailed mechanism of H/H^+ stabilization depends on the structural and electronic properties of the adsorption site. The strongest binding occurs with the oxygen O(c) bridging two bare vanadium atoms. These O(c) oxygens become quite mobile in presence of the H/H^+ adparticle. Oxidation of propene and toluene on V_2O_5(0 1 0) into the aldehyde species proceeds through the formation of C–O bond with the bridging oxygen, abstraction of two hydrogen atoms from the same carbon atom of CH_3-group, and generation of two OH-surface groups.

Keywords: V_2O_5; Electronic structure; Cluster model calculations; Hydrogen adsorption and hydrocarbons interaction with V_2O_5

1. Introduction

The understanding of catalytic processes occurring on transition metal oxide surfaces requires a complete characterization of physical and chemical properties of the surface, information on the transition complex which is formed at the surface, and insight into the reaction between the adsorbates. The electronic structure of the surface is responsible for the interaction and binding with an adsorbate, for resulting bond changes, for the reaction of adsorbed reactant(s), and for the

*Corresponding author. Tel.: +48-12-4252841; fax: +48-12-4251923; e-mail: mcwitko@cyf-kr.edu.pl

0920-5861/99/$ – see front matter
PII: S0920-5861(98)00490-8

desorption process. Therefore, one has to determine which atoms act as active centers directing the transformation of the reagent and how the properties of an active center depend on its geometrical and chemical arrangements. Further, it is necessary to learn how binding in the intermediate complex (composed of the reacting molecule and a group of atoms of the catalyst forming the active environment) modifies the electronic structure of the molecule and influences the reactivity of different bonds, thus determining the type of product. Recent developments in surface experimental techniques [1] give access to a wide spectrum of information concerning details of catalytic reactions on both atomic and electronic levels. On the other hand, rapid advances in methodology and in computer performance provide various theoretical approaches (quantum chemical and/or solid state physics based), which can be used as parallel or complementary tools to study elementary steps of catalytic processes.

All theoretical treatments of catalytic systems are based on model assumption addressing three different aspects [2]. First, the geometric structure of the local system where the catalytic reaction happens has to be defined. Second, the electronic interaction between the atoms of the local system has to be treated in a theoretically satisfactory and numerically adequate manner. Third, the electronic coupling of the local system to its substrate environment has to be accounted for. The quality of theoretical results and their relevance with respect to experimental data for real catalytic systems is determined by basically two approximations, those used to simplify the system geometry and those used to evaluate the electronic structure of the model system. Obviously, both approximations influence each other and there are no simple criteria to select cluster geometries or theoretical methods to yield a given accuracy for the comparison with experimental results. When choosing local clusters to model the surface, one has to examine different clusters varying in size and shape in order to assess cluster size convergence resulting in the reasonable surface representation. Further, systematic studies using different electronic structure methods (which are complementary in nature) are needed to obtain a complete electronic description of the catalytic model system.

The interest in the electronic structure of vanadium oxide surfaces originates from the wide application of vanadia based materials as catalysts, especially in the selective oxidation of hydrocarbons (aliphatic as well as aromatic) [3,4]. The existence of the structurally (and thus electronically) different oxygen sites on the V_2O_5(0 1 0) surface poses the question as to which of these sites is involved in the different elementary steps of the oxidation reaction. In particular, it is interesting to ask which surface oxygen sites are responsible for the activation of C–H bonds (abstraction of hydrogen) in a hydrocarbon reactant near the surface and which oxygen is being inserted into the organic molecule (yielding the oxygenated product). Many microscopic details of these processes (which involve adsorption and surface bond breaking/making) are still under discussion and require more experimental as well as theoretical work.

The electronic structure of vanadium pentoxide(0 1 0) surface as well as adsorption at this surface have been examined previously [5–15] in different cluster model studies using ab initio Hartree–Fock [5–7] and density functional theory (DFT) [8,9] as well as semiempirical INDO [10–13] and charge sensitivity analysis [14,15] approaches. All these studies have been performed using an idealized V_2O_5(0 1 0) surface geometry with averaged interatomic V–O distances and O–V–O angles. The results show pronounced differences between structurally different oxygen sites present at the V_2O_5(0 1 0) surface. It is found that bridging oxygen sites are more negatively charged than terminal (vanadyl) sites. Further, hydrogen/proton adsorption at the different oxygen sites results always in strong binding and surface OH formation. However, OH groups deriving from doubly coordinated bridging oxygen sites at V_2O_5(0 1 0) can become mobile and can desorb from the surface whereas terminal OH groups forming above vanadium centers are very tightly bound.

In the following, the electronic structure of the vanadium pentoxide(0 1 0) surface is discussed based upon quantum chemical calculations carried out for V–O clusters of various sizes and geometries up to $V_{38}O_{116}H_{42}$. For $V_2O_9H_8$, $V_{10}O_{31}H_{12}$ and $V_{16}O_{49}H_{18}$, the results of a semiempirical ZINDO [16–18] treatment are compared with those of ab initio density functional theory (DFT) method [19]. The study of the largest $V_{38}O_{116}H_{42}$ cluster allows us to discuss also the effect of (weak) inter-layer coupling between the first and second surface layer on the electronic proper-

ties of V_2O_5(0 1 0). In addition, the $V_{10}O_{31}H_{12}$ surface cluster of idealized geometry is compared with that where the surface geometry is represented by bulk termination using experimental crystallographic data as well as with the cluster whose geometry has been optimized locally. Such a systematic comparison can help to elucidate the effect of idealizing the surface geometry and to define appropriate clusters representing physical and chemical properties is the real V_2O_5(0 1 0) surface. The catalytic properties of vanadium pentoxide are examined by analyzing its interaction with a proton and selected aliphatic and aromatic hydrocarbons. Further, elementary steps of the selective oxidation of propylene and toluene molecules on vanadium pentoxide catalysts will be discussed.

2. Electronic structure of V_2O_5 surface clusters

The crystal lattice of vanadium pentoxide, V_2O_5, is of orthorhombic symmetry with a space group D_{2h}-P_{mmn} and unit cell parameters defined as a=11.51 Å, b=4.37 Å, c=3.56 Å [20–22]. The building unit of V_2O_5 forms a distorted octahedron with V–O bond distances varying between very short (1.58 Å, vanadyl groups) and very long values (2.79 Å, Van der Waals type bonding), see. Fig. 1(a). Because of these significant distance differences, the coordination of the vanadium may be regarded as tetragonal, square pyramidal or octahedral depending on the extent of the first coordination sphere. Assuming octahedral coordination, each of the oxygens of the vanadyl group (with shortest V–O bond) is also connected by a very long *trans*-bond with a neighboring vanadium. This geometry results in a layer structure with an easy cleavage plane perpendicular to the *b*-axis ((0 1 0) direction). The lattice of vanadium pentoxide may also be described by zig-zag chains of edge-sharing octahedra running along the *c*-axis and crosslinked by shared oxygen corners to form infinite layers in the *ac*-plane, see Fig. 1(b). Adjacent layers are connected (along the *b*-direction) by oxygen corners involving both very long and very short V–O distances, see Fig. 1(c). Therefore, the catalytically active (0 1 0) surface of V_2O_5 can be discussed in terms of distorted edge and corner-linked square pyramids. This surface contains three structurally different oxygen sites,

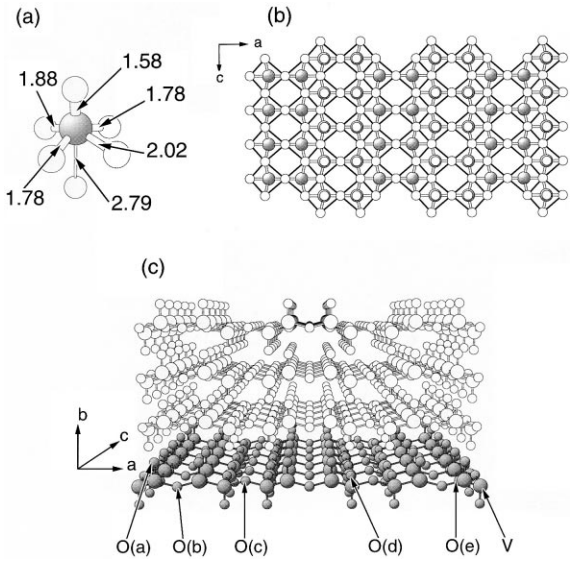

Fig. 1. Crystallographic structure of orthorhombic V_2O_5. Part (a) shows an elementary VO_6 octahedron with all inequivalent V–O distances given in Å. Part (b) shows the geometric structure of the (0 1 0) crystal plane of V_2O_5 where V(O) centers are included as shaded (white) balls. Part (c) gives a perspective view of the three-dimensional lattice with the (0 1 0) crystal plane emphasized by shaded balls. The different surface oxygen sites O(a–e) are labeled accordingly.

vanadyl oxygens coordinated to one vanadium, O(1) and bridging oxygens coordinated to two O(2) or three O(3) vanadium atoms. The situation is more complex when the molecule approaching the surface is involved. In this case, one has to distinguish five structurally inequivalent surface oxygens O(a–e), the vanadyl oxygen O(a)=O(1), coordinated to one vanadium, bridging oxygens O(b,c)=O(2) coordinated to two vanadiums, where O(b) bridges two vanadyl groups, whereas O(c) connects two bare vanadium atoms, and bridging oxygens O(d,e)=O(3) coordinated to three vanadiums but involving vanadyl groups with different orientations, see Fig. 1(c).

In the following, the (0 1 0) surface of V_2O_5 is modeled by clusters of finite size where the electronic structure and respective geometry optimizations are determined by the semiempirical ZINDO [16–18] and ab initio DFT [19,23] methods. Local electronic properties near the different surface oxygen sites are analyzed with the help of Mulliken populations and Meyer bond-order indices.

2.1. V_2O_5 surface clusters with idealized geometry

The idealized structure of vanadium pentoxide is obtained from the crystallographic structure by averaging all V–O distances and O–V–O angles of bridging oxygens within the (0 1 0) layers, resulting in d(V–O)=1.89 Å and <(OVO)=86.16°, while for the distances of terminal vanadyl oxygens the crystallographic bulk value, d(V–O)=1.58 Å is used. The layers of the idealized structure exhibit inversion, twofold rotational and mirror symmetry. These symmetries are used to construct finite layer sections of increasing size about a given oxygen center resulting in clusters V_2O_9, $V_{10}O_{31}$, $V_{16}O_{49}$ describing one layer (see Fig. 2(a)) and $V_{38}O_{116}$ ($V_{24}O_{71}$+$V_{14}O_{45}$) referring to two adjacent layers (see Fig. 2(b)). Embedding of the clusters into their surface environment is achieved by saturating dangling bonds of peripheral oxygen atoms by hydrogen atoms and leads to $V_2O_9H_8$, $V_{10}O_{31}H_{12}$, $V_{16}O_{49}H_{18}$, and $V_{38}O_{116}H_{42}$ clusters.

Due to their inversion symmetry, the present clusters can be used to model different local environments at the V_2O_5(0 1 0) surface depending on which side of the cluster, top or bottom, is considered. As an illustration, the $V_2O_9H_8$ cluster (Fig. 2(a)) forms a symmetric environment about the doubly coordinated oxygen O(2) and is defined as the O(b) site on V_2O_5(0 1 0) surface when viewed from above or as the O(c) site when viewed from below. Similarly, in the larger clusters O(d) and O(e) sites (both triply coordinated O(3)) can be treated equivalently. This symmetry behavior will be made use of in the following discussion of different surface oxygen sites. The $V_2O_9H_8$ cluster shown by the dark gray area of Fig. 2(a) is the smallest cluster to give a meaningful description of the surface oxygen sites O(a–c), while the larger clusters, $V_{10}O_{31}H_{12}$ and $V_{16}O_{49}H_{18}$, form symmetric environments about the O(b,c) sites but are large enough to account also for the O(d,e) sites in a reasonable way.

Table 1 summarizes the results of Mulliken population and bond order analyses for $V_2O_9H_8$, $V_{10}O_{31}H_{12}$, and $V_{16}O_{49}H_{18}$ clusters modeling the first V_2O_5(0 1 0) surface layer as well as for $V_{38}O_{116}H_{42}$ representing the first and second surface layer. In addition, this table contains energy values of the highest occupied orbitals (HOMO) in the clusters. For $V_2O_9H_8$, $V_{10}O_{31}H_{12}$, and

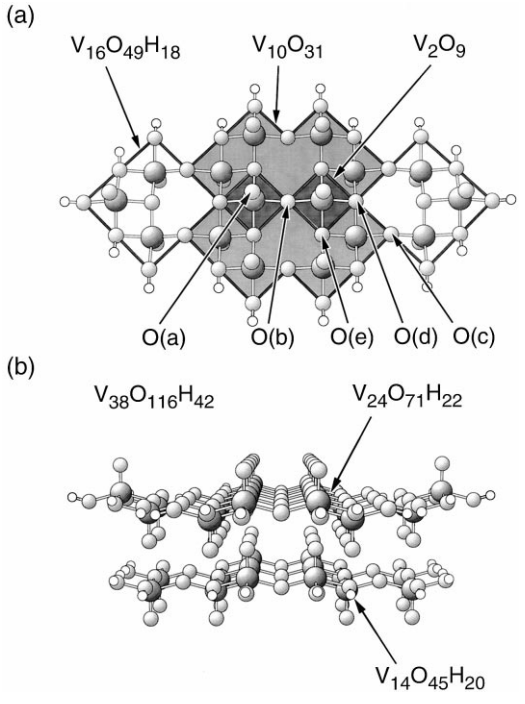

Fig. 2. Balls and sticks model describing the geometry of V_2O_5(0 1 0) substrate clusters $V_nO_mH_k$ used in the present study. Here V(O) centers are shown as dark (light) shaded balls and H-terminator atoms as small white balls. Part (a) shows all one-layer clusters, $V_2O_9H_8$, $V_{10}O_{31}H_{12}$, and $V_{16}O_{49}H_{18}$, where the gray shaded background illustrates the building sequence. Note that H-terminator atoms are included only for the largest cluster. Part (b) gives a perspective view of the two-layer cluster $V_{38}O_{116}H_{42}$ together with its decomposition into layer components $V_{24}O_{71}H_{22}$ (upper layer) and $V_{14}O_{45}H_{20}$ (lower layer), respectively.

$V_{16}O_{49}H_{18}$ clusters, the ZINDO results are compared with those of DFT method. As expected, the vanadium atoms are always ionic with their positive charges amounting to 1.15 on the average (from both methods). All oxygens form negative ions where the bridging oxygens O(b–e) carry more negative charge (−0.46/−0.56 averaged ZINDO/DFT values) than the vanadyl oxygens O(a) (−0.36/−0.30 averaged ZINDO/DFT values). Among bridging oxygens, the triply coordinated O(3)=O(d,e), become slightly more negative than the doubly coordinated O(2)=O(b,c). While the charge differences between different types of oxygens are smaller in the ZINDO than in the DFT approach, the results based on the semiempirical ZINDO method are in qualitative agreement with previous ab initio HF

Table 1
Results of Mulliken population analysis for the $V_2O_9H_8$, $V_{10}O_{31}H_{12}$, $V_{16}O_{49}H_{18}$, and $V_{38}O_{116}H_{42}$ clusters

	$V_2O_9H_8$ (ZINDO/DFT)	$V_{10}O_{31}H_{12}$ (ZINDO/DFT)	$V_{16}O_{49}H_{18}$ (ZINDO/DFT)	$V_{38}O_{116}H_{42}$ ($V_{24}O_{71}H_{22}/V_{14}O_{45}H_{20}$ (ZINDO))
Q(V)	1.20/0.98	1.08/1.26	1.08/1.26	1.11/1.08
Q(O(a))	−0.40/−0.29	−0.37/−0.26	−0.38/−0.26	−0.39/−0.39
Q(O(b,c))	−0.44/−0.51	−0.45/−0.55	−0.45/−0.55	−0.45/−0.45
Q(O(d,e))	–	−0.48/−0.71	−0.47/−0.73	−0.47/−0.48
P(V–O(a))	2.51/2.17	2.53/2.17	2.53/2.16	2.51/2.52
P(V–O(b,c))	1.11/0.97	1.10/0.91	1.10/0.90	1.08/1.10
	1.11/0.97	1.10/0.91	1.10/0.90	1.08/1.10
P(V–O(d,e))	–	0.82/0.59	0.83/0.58	0.80/0.79
	–	0.76/0.50	0.76/0.49	0.79/0.84
	–	0.84/0.59	0.84/0.58	0.83/0.79
HOMO[eV]	−8.25/−5.54	−9.17/−6.64	−8.79/−6.58	−8.19

The atom charges Q, refer to vanadium and oxygen atoms closest to the cluster center. For each type oxygen (single coordinated O(a), double coordinated O(b,c) and triple coordinated O(d,e)) P(V–O) denotes the bond order with the nearest vanadium atom. The table contains in addition energies of the highest occupied orbital (HOMO) of each cluster.

and DFT data [5–9]. The discrepancy is partly due to different basis representations of the valence orbitals.

In addition to ionic V–O bonding reflected by the different atom charging in the system, the V–O interaction contains covalent contributions which can be characterized by respective bond order indices P(V–O). The value P(V–O(a)) describing the bond of a vanadium atom with its terminal (vanadyl) oxygen O(1) amounts to about 2 which confirms the strong vanadyl double bond. The bond orders P(V–O(b,c)) characterizing the bond of a doubly coordinated bridging oxygens O(2) with each of its neighboring vanadium atoms is found to be about 1 which indicates two single V–O bonds. Further, the calculations yield P(V–O(d,e))=0.81/0.64 (averaged ZINDO/DFT values) for each of the V–O bonds of a triply coordinated oxygen atoms O(3) suggesting three weaker than single bonds. Taking the sum of respective bond orders as a measure of the stability of the different oxygen sites which can participate in surface reactions, the above results indicate that the oxygens coordinated to two vanadium atoms can be most easily removed from the surface.

The influence of the second surface layer on the electronic structure of the V_2O_5(0 1 0) surface is studied by the $V_{38}O_{116}H_{42}$ cluster which consists of $V_{24}O_{71}H_{22}$ (1st layer) and $V_{14}O_{45}H_{20}$ (2nd layer) subclusters, see Fig. 2(b). Previous semiempirical SINDO calculation [24] emphasized the importance of the second layer for the surface electronic structure of V_2O_5(0 1 0) and yielded an optimized inter-layer distance which is smaller than the bulk value by 0.5 Å. However, the present inter-layer distance optimization in the $V_{38}O_{116}H_{42}$ cluster leads to a value which differs from the bulk result by only 0.2 Å. Further, Table 1 shows unequivocally that the presence of the second layer does not affect the electronic structure of the first layer and can therefore be neglected for the electronic structure of V_2O_5(0 1 0) surface. Atomic populations and bond orders of the two different layers in $V_{38}O_{116}H_{42}$ yield only very small differences.

The highest occupied orbitals (HOMO) of the present clusters are identified as O 2p type referring to doubly coordinated bridging surface oxygen atoms. Their one-electron energies vary within a range of 8.2–9.2 eV (ZINDO method) and 5.5–6.5 eV (DFT method), respectively, as a function of cluster size, see Table 1. These energies can be interpreted as Koopmans ionization potentials which are expected to converge to the surface workfunction for infinite cluster size. In view of the limited size of the present clusters and the approximations used for the electronic structure determination (the ZINDO approach, in particular), the calculated values compare reasonably well with the experimental data of the work function for V_2O_5(0 1 0) amounting to 6.712±0.083 eV [25]

The results of both semiempirical and DFT treatments indicate that size convergence of the electronic properties of the V_2O_5(0 1 0) surface is achieved for clusters as large as $V_{10}O_{31}H_{12}$ and that both semiempirical and DFT approaches yield qualitatively identical results. Therefore, in the following, the $V_{10}O_{31}H_{12}$ cluster is used to illustrate differences in the electronic structure between the idealized surface geometry and that taken from the measured bulk crystallographic lattice. The calculations reported in the following are based upon the ZINDO method.

2.2. V_2O_5 surface clusters with bulk geometry

In order to study the influence of atom displacements on the electronic structure of the V_2O_5(0 1 0) surface, ZINDO calculations are performed for $V_{10}O_{31}H_{12}$ cluster in its idealized geometry discussed above and in its experimental bulk terminated surface geometry taken from crystallographic data. The latter geometry will be denoted in the following by ''bulk geometry''. The difference between the two cluster geometries is shown in Fig. 3, where dark shaded balls describe the idealized structure (averaged V–O distances and O–V–O angles) and white balls refer to the bulk geometry. The V–O distances of singly coordinated terminal oxygens O(a)=O(1) (d(V–O)=1.58 Å) do not differ between the idealized and bulk geometry, whereas d_{V-O} for doubly coordinated bridging oxygens, O(b,c)=O(2), is shorter (1.78 Å) for the bulk compared to the idealized structure (1.89 Å). Further, in the bulk geometry triply coordinated bridging oxygens, O(d,e)=O(3), are bonded to vanadium atoms at distances of 1.88 Å close to the averaged value and to one vanadium atom at a larger distance (2.02 Å). The comparison in Fig. 3 shows also that the relative atom displacements between the two geometries increase in going from the cluster center to the periphery which is expected since the two surface geometries are required to coincide in the cluster center.

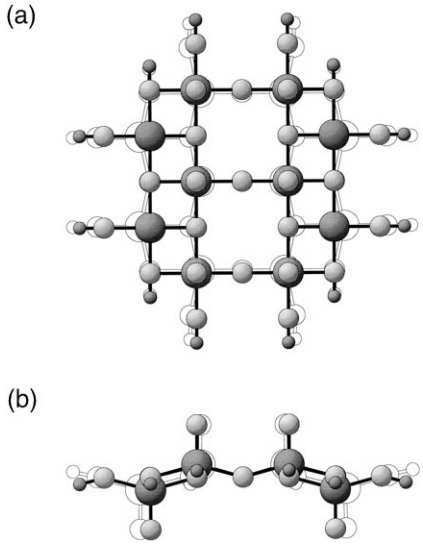

Fig. 3. Geometric structure of the $V_{10}O_{31}H_{12}$ substrate cluster illustrating the idealized (shaded balls) and the bulk terminated (white balls) geometry of the V_2O_5(0 1 0) surface. In the comparison, the cluster centers of the two geometries are allowed to coincide. The cluster geometries are shown for views along the (a) (0 1 0) and (b) (0 0 1) direction.

Table 2 contains results of the Mulliken population and bond order analyses for the $V_{10}O_{31}H_{12}$ cluster, where values calculated for the idealized geometry are compared with those of the bulk geometry. Obviously, there are no sizable differences in the atom charges obtained for the two geometries. The V–O bond orders differ only slightly between the two geometries and reflect the general trend, where increasing the bond distance results in a decreased bond order value. Thus, in the bulk geometry cluster doubly coordinated oxygens O(b,c)=O(2) show an increased bond order P(V–O(b,c))=1.21 compared to that of the idealized geometry (1.10) which is consistent with the decreased interatomic V–O distance and suggests stronger V–O bonding in the bulk geometry. Bond orders P(V–O(d,e)) of the triply coordinated oxygens describing bonds with their three individual V-neighbors vary also for both geometries according to the different V–O distances. However, the compound bond order summed over all V-neighbors of O(d,e)=O(3) and characterizing the total bond strength of these oxygens does not differ between the idealized and the bulk geometry cluster.

2.3. V_2O_5 surface clusters with optimized geometry

The surface cluster approach uses local clusters that are described by finite surface sections cut out of the real substrate. This implies, in particular, that the equilibrium geometry of the finite size cluster reflects

Table 2
Mulliken population and Meyer bond order results of the $V_{10}O_{31}H_{12}$ substrate cluster in its idealized, bulk, and optimized geometry

	Idealized geometry	Bulk geometry	Optimized geometry
Q(V)	1.08	1.08	0.93
Q(O(a))	−0.37	−0.38	−0.33
Q(O(b,c))	−0.45	−0.46	−0.43
Q(O(d,e))	−0.48	−0.48	−0.40
P(V–O(a))/d(V–O(a))	2.53/1.58	2.53/1.58	2.61/1.58
P(V–O(b,c))/d(V–O(b,c))	1.10/1.89	1.21/1.78	1.20/1.89
	1.10/1.89	1.21/1.78	1.20/1.89
	0.83/1.89	0.90/1.88	0.84/2.11
P(V–O(d,e))/d(V–O(d,e))	0.76/1.89	0.86/1.88	0.81/2.14
	0.84/1.89	0.68/2.02	0.74/2.20

The atom charges Q, refer to vanadium and oxygen atoms closest to the cluster center. For each type oxygen (single coordinated O(a), double coordinated O(b,c) and triple coordinated O(d,e)) P(V–O) denotes the bond order with the nearest vanadium atom. The table contains in addition values of respective V–O binding distances (in Å).

that of the local section at the real surface. This approximation and its consequences for the local surface electronic structure as well as reactivity can be tested by separate geometry optimizations carried out for the free surface cluster. Therefore, the $V_{10}O_{31}H_{12}$ cluster geometry is reoptimized such that all atoms are allowed to rearrange. Both the idealized and bulk geometry of the cluster are used as starting points and yield, as expected, the same final optimized geometry.

Fig. 4 compares the result of the cluster optimization (optimized geometry, dark shaded balls) with the bulk geometry (white balls) and Table 2 lists respective V–O bond distances. Obviously, the optimization leads to sizable changes in all atom positions and interatomic distances. The cluster surface assumes a warped shape that indicates a tendency towards more compact cluster geometry. The V–O distances involving all bridging oxygens increase, while the vanadyl bond distances remain unchanged in comparison with the bulk geometry. Table 2 contains also atom charges and bond orders obtained for the optimized cluster geometry. A comparison with the results of the bulk geometry shows that all atoms of the optimized cluster are slightly less ionic while there are no obvious differences in the bond order values. This suggests that the relative importance of ionic contributions to interatomic bonding is reduced in the optimized geometry vs. the bulk geometry cluster, while changes due to covalent binding are found to be rather small.

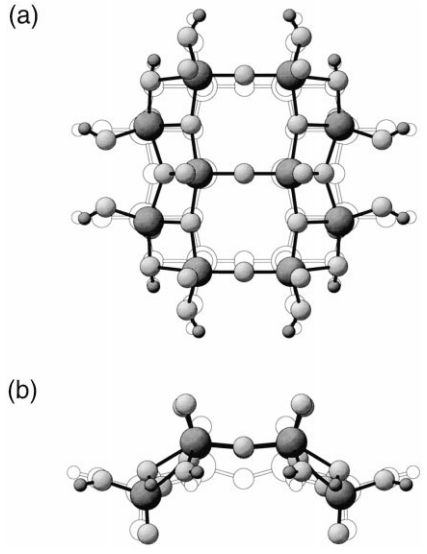

Fig. 4. Geometric structure of the $V_{10}O_{31}H_{12}$ substrate cluster illustrating the bulk terminated (white balls) and the fully optimized (shaded balls) geometry, see text. In the comparison, the cluster centers of the two geometries are allowed to coincide. The cluster geometries are shown for views along the (a) (0 1 0) and (b) (0 0 1) direction.

In summary, the present cluster model calculations can give a clear picture of the electronic structure and binding at the (0 1 0) surface of vanadium pentoxide. The calculations yield electronic properties that are converged with respect to cluster size for clusters as

large as $V_{10}O_{31}H_{12}$ (see [5–9,26,27]). All electronic parameters of the $V_{10}O_{31}H_{12}$ cluster in its idealized, bulk and optimized geometry are found to be rather similar which indicates that the electronic properties of the V_2O_5(0 1 0) surface can be safely described by the cluster in its idealized geometry. This cluster is computationally attractive due to its symmetry properties. Further, the neglect of the second surface layer of V_2O_5(0 1 0) in $V_{10}O_{31}H_{12}$ has been demonstrated to be of minor importance. The electronic binding in vanadium pentoxide is described by both ionic and covalent contributions. Further, the calculations reveal clear electronic differences between structurally different surface oxygen sites. Bridging oxygen sites are always found more negatively charged than terminal (vanadyl) oxygen sites. This suggests an increased local reactivity of bridging oxygen centers with respect to electrophilic attack. Electrostatic potentials near the V_2O_5(0 1 0) surface, discussed elsewhere [8,9], yield negative minima above the bridging oxygen sites, while there are no pronounced maxima above the surface vanadium centers. Therefore, reactions of nucleophilic adparticles with the surface seem to be less probable than reactions of electrophilic species.

3. Adsorption of H/H^+ at the V_2O_5(0 1 0) surface

Hydrocarbon oxidation at transition metal oxide surface consists of several steps such as activation of the C–H bond (abstraction of hydrogen) in the reactant molecule and insertion of oxygen into the species (yielding the oxygenated product). An understanding of all mechanisms of this catalytic reaction requires detailed knowledge of geometric and electronic parameters determining the processes. In particular, it is important to find out which of the structurally inequivalent oxygen centers at the oxide surface is involved in which elementary process. In order to model the behavior of H/H^+ species which is split off by the C–H activation near the V_2O_5 surface, the adsorption of hydrogen at different oxygen sites can be discussed. This reaction has been considered earlier in semiempirical as well as ab initio studies of small $V_2O_9H^+$ ($V_2O_9+H^+$) [5–7] and $V_2O_9H_8H^+$ ($V_2O_9H_8+H^+$) [8,12,13] clusters discussing the reactivity of O(a–c) surface oxygen sites as well as in ZINDO [13,26] and ab initio DFT [8,9] studies on the $V_{10}O_{31}H_{13}{}^+$ ($V_{10}O_{31}H_{12}+H^+$) cluster, where all inequivalent oxygen sites O(a-–e) were taken into consideration. The influence of the substrate geometry on H/H^+ adsorption was discussed in Ref. [26], where adsorption at different sites of $V_{10}O_{13}H_{12}$ cluster in its idealized and bulk geometry was compared. Here we summarize only briefly the results of the calculations which are important for the following discussion concerning the interaction of hydrocarbon molecules with the V_2O_5(0 1 0) surface.

The H/H^+ species adsorbs at the V_2O_5(0 1 0) surface always at oxygen sites forming very stable surface hydroxyl groups. The detailed mechanism of the stabilization depends on the structural and electronic properties of the adsorption site. The strongest binding occurs with the doubly coordinated oxygen O(c) bridging two bare vanadium atoms which is identified as the strongest nucleophilic site. Test calculations with the H/H^+ adparticle kept fixed above the surface show that the O(c) oxygens become quite mobile in presence of the adparticle. Allowing the surface oxygens to relax during adsorption of H/H^+ leads to different adsorption scenarios depending on the surface oxygen site. At the terminal vanadyl oxygen site, a very stable and rigid hydroxyl group O(a)H is formed above the vanadium center. At the doubly coordinated oxygen site O(b), the H/H^+ adsorbate penetrates between two vanadyl groups to form a local O(b)H group while at the O(c) site, an O(c)H group is created slightly above the surface O(c) position with O–H binding being strongest. Weak initial interaction between triply coordinated oxygens O(d,e) and the incoming H/H^+ species leads to stabilization of the adsorbate near the closest vanadyl site resulting in a tilted O(a)H group instead of O(d)H or O(e)H. The formation of the surface hydroxyl groups leads to a significant weakening of the respective V–O bonds, with the weakening being strongest for V–O(c)–V bonds. This may indicate that the hydrogen abstracted from the hydrocarbon molecule may adsorb at all surface oxygen sites. However, its adsorption above doubly coordinated oxygens O(c) will lead to a strong weakening of the V–O(c)–V bonds and, as a result, this bridging oxygen will be inserted into the hydrocarbon molecule (yielding the oxygenated product) with highest probability.

4. Interaction of propene with the V_2O_5(0 1 0) surface

Selective oxidation of aliphatic hydrocarbons (e.g., propene, C_3H_8) involves dehydrogenation and oxygen insertion processes [28–30]. On a typical catalyst (e.g. molybdate), the molecule is activated by the abstraction of hydrogen from an α position (H_α) with respect to the C=C double bond. As the next step, the nucleophilic attack of oxygen on the allylic species takes place simultaneously with the abstraction of a second hydrogen atom. This step leads to the formation of an adsorbed acrolein molecule which has to desorb from the surface. The abstraction of H_α and formation of a symmetric allylic species (with both terminal carbon atoms being equally available for conversion into the carbonyl group of acrolein) has been confirmed by several authors using labeled propene [31–33]. Direct evidence of the generation of allylic species as an intermediate was provided also by the IR spectra of propene adsorbed on catalysts used for partial and total oxidation [34–36]. The results of the experiments based upon the idea of bypassing the first rate determining step of the reaction (by generating the allyl radical in situ in a catalytic reactor [37,38]) enable the identification of those catalyst centers which are responsible for the propene activation and those involved in the insertion of oxygen. Theoretical studies of the individual steps of the propene oxidation process were discussed in Refs. [39–46]. Here, we analyze the interaction of propene with the V_2O_5(0 1 0) surface and compare with the mechanisms on a typical oxidative catalysts (molybdates). This stresses again the role of structurally different surface oxygen ions participating in the elementary processes.

In studies concerning the interaction of propene with the V_2O_5(0 1 0) surface [13,47], it was found that the product of the oxidation reaction strongly depends on the relaxation of oxygen atoms in the cluster. If none of the surface oxygens are allowed to relax during the propene approach, the reaction does not take place. The relaxation of one single oxygen adsorption site leads to the alcohol-like species, whereas relaxing more surface oxygen centers results in formation of a precursor of aldehyde and two surface hydroxyl groups. The reaction on the cluster containing only one vanadium center differs from the reaction on clusters which have more than one vanadium atom. On the former, the precursor of alcohol is obtained whereas on the latter, the reaction leads to the precursor of acrolein. The calculations of the reaction pathway [47] in which the optimization of propene as well as of all nearest surface oxygen atoms were performed indicate that the reaction proceeds in a step-wise fashion. It starts with C–O bond formation followed by abstraction of two hydrogen atoms from the methyl group. In the following we restrict the discussion to the interaction of a propene molecule with the $V_{10}O_{31}H_{12}$ cluster.

The propene molecule approaches perpendicular to the V_2O_5(0 1 0) plane with the methyl group pointing towards the oxygen O(c) coordinated to two bare vanadium atoms in the $V_{10}O_{31}H_{12}$ cluster. In this approach, the optimization of propene as well as all surface oxygen atoms is carried out. The results of the present calculations are summarized in Table 3 which contains the changes of selected bonds within the organic molecule and in the substrate cluster due to the reaction. In addition, Fig. 5 shows the structures of the reactants (the isolated propene and the cluster, Fig. 5(a)) and the product (precursor of the aldehyde,

Table 3
Results for the interaction of propene with $V_{10}O_{31}H_{12}$ cluster

A–B bond	Substrate (R(A–B)[Å]/P(A–B))	Product (R(A–B)[Å]/P(A–B))
C1–C2	1.33/1.98	1.34/1.90
C2–C3	1.47/1.06	1.35/1.06
C3–O(c)	–	1.36/1.75
C3–H/C3–H	1.10/0.98	1.37/0.94
C3–H/O–H	1.11/0.96	1.09/0.78
V–O(c)	1.89/1.10	2.55/0.16

Selected bond distances R(A–B) [Å] and bond order indices P(A–B) for the isolated species (substrate) and transition complex (product) are given.

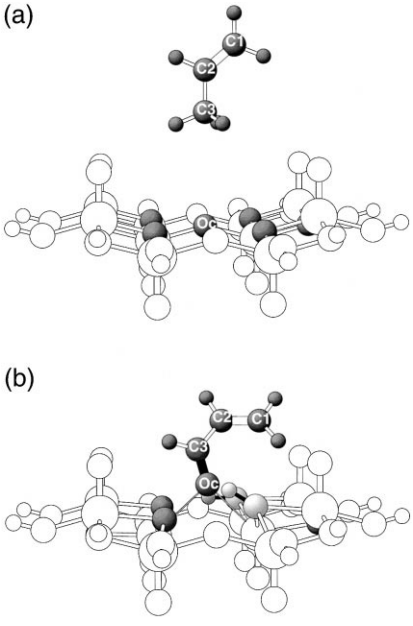

Fig. 5. Interaction of propene with the $V_{10}O_{31}H_{12}$ cluster. The O, C and H atoms whose position are allowed to relax are denoted as shaded balls and labeled. Part (a) gives a starting geometry for the interaction (the organic molecule approaches the cluster in the direction perpendicular to the plane of the cluster, the CH_3-group pointing the bridging oxygen O(c). Part (b) shows a final product (precursor of an aldehyde). The C–O bond and two O–H surface hydroxyl groups (both between the H from the methyl group and triply coordinated O(d)) are shown in black.

Fig. 5(b)) of the studied reaction. The interaction of propene with the cluster creates two double bonds within the organic molecule, the double C=C bond (P(C–C)=1.90) and the C=O bond (P(C–O)=1.75) between the carbon atom of the methyl group and the doubly coordinated surface oxygen. This process is equivalent to the formation of the adsorbed acrolein species. The surface oxygen atom, (O(c)), which is inserted into the organic molecule weakens its binding with the neighboring vanadium atoms (P(V–O)=0.16 in contrast to P(V–O)=1.10 for the isolated cluster). The abstraction of hydrogen atoms from the methyl group results in two surface hydroxyl groups with triply coordinated oxygen sites which weaken the bond between the vanadium atom and the O(d) oxygen atom (P(V–O)=0.50/0.55/0.39 in contrast to P(V–O)=0.82/0.76/0.84 for the isolated cluster). The formation of an aldehyde is connected with the reduction of two vanadium atoms bound to the oxygen site O(c) and involved in the reaction (Q(V)=+0.48/0.65 while Q(V)=+1.08 in the isolated cluster). The neutral charge of the final species suggests an aldehyde precursor which can easily desorb leaving the oxygen vacancy behind. The mechanism of the propene oxidation on the V_2O_5(0 1 0) surface differs from that on typical catalysts since it does not start with a symmetric allylic species, but with an alkoxy species.

5. Interaction of toluene with the V_2O_5(0 1 0) surface

The oxidation of aromatics may involve the side-chain (without affecting the π-electron system of the aromatic ring) or the π-electron system of the aromatic ring (without affecting the side-chain). The first reaction proceeds according to the nucleophilic mechanism and yields aldehydes and acid or anhydrides. The second proceeds along the electrophilic route and results in acid anhydrides [48]. In the case of toluene (C_7H_8) molecules, both reactions may take place. Oxidation of toluene on vanadium oxide monolayers has been a subject of many experimental studies (see [48,49] and references therein). The elucidation of the mechanism of this reaction leads to the conclusion that the reaction starts with a benzyl intermediate which interacts with surface lattice oxygen to form, consecutively, adsorbed benzaldehyde and benzoic acid precursors. These may desorb as products of a selective nucleophilic oxidation, may be further oxidized to carbon oxides, or undergo degradation of the aromatic ring with the formation of maleic anhydride and carbon oxides.

The interaction of toluene with the small clusters modeling the V_2O_5(0 1 0) surface was already discussed in [50,51]. It was found that the adsorption with the ring plane parallel to the plane of the cluster is the most exothermic. However, such an adsorption results in strong interactions of carbon atoms with surface vanadium and oxygen atoms creating carbon deposit or total oxidation products. Perpendicular end-on adsorption of toluene with methyl group pointing towards the bridging oxygen leads to abstraction of two hydrogen atoms from the methyl group and results in strong carbon–oxygen bonds to yield the precursor of benzaldehyde. Here, we discuss only the interaction of toluene with the $V_{10}O_{31}H_{12}$ cluster.

Table 4
Results for the interaction of toluene with $V_{10}O_{31}H_{12}$ cluster

A–B bond	Substrate (R(A–B) [Å]/P(A–B))	Product (R(A–B) [Å]/P(A–B))
C1–C2	1.47/1.04	1.43/0.86
C2–O(1)	–	1.44/1.54
C1–H/C1–H	1.10/0.98	1.45/0.69
C1–H/O–H	1.11/0.97	1.46/0.81
V–O(c)	1.89/1.10	1.47/0.47

Selected bond distances R(A–B) [Å] and bond order indices P(A–B) for the isolated species (substrate) and transition complex (product) are given.

In the model calculations, the toluene molecule is assumed to approach the $V_{10}O_{31}H_{12}$ cluster end-on with the carbon of the methyl group pointing towards the oxygen bridging two bare vanadium atoms. During the approach, the geometry of the toluene molecule as well as of all surface oxygen atoms is optimized. The results are summarized in Table 4 which contains the changes of selected bonds within the organic molecule and in the substrate cluster due to the reaction. In addition, Fig. 6 shows the structures of the reactants (the isolated toluene and the cluster, Fig. 6(a)) and of the product (precursor of aldehyde, Fig. 6(b)). The mechanism of forming the aldehyde species is similar to that of propene where the reaction proceeds stepwise. It starts with C–O bond formation and is followed by abstraction of two hydrogen atoms from the methyl group which occurs only at very short C–O distances. The resulting aldehyde species is almost neutral and is expected to desorb leaving an oxygen vacancy behind. The bond order of the C=O bond amounts to 1.54. The bond orders of the C–C bonds in the aromatic ring do not change if compared with the isolated toluene molecule and are equal to 1.44. The binding of the surface oxygen atom (which is inserted into the organic molecule) with the vanadium atom is weakened (P(V–O)=0.47 compared to P(V–O)=1.10 in the isolated cluster). The abstraction of hydrogen atoms from the methyl group results in two surface hydroxyl groups with triply coordinated oxygen atoms which weaken the bond between the three vanadium atoms and the oxygen atom O(d) (P(V1,2,3-O)=0.38/0.47/0.48 compared to P(V1,2,3-O)=0.82/0.76/0.84 in the isolated cluster). The formation of the aldehyde is connected with the reduction of the two vanadium atoms bound to the oxygen site O(c) and involved in the reaction (Q(V)=+0.64/0.16 compared to Q(V)=+1.08 in the isolated cluster).

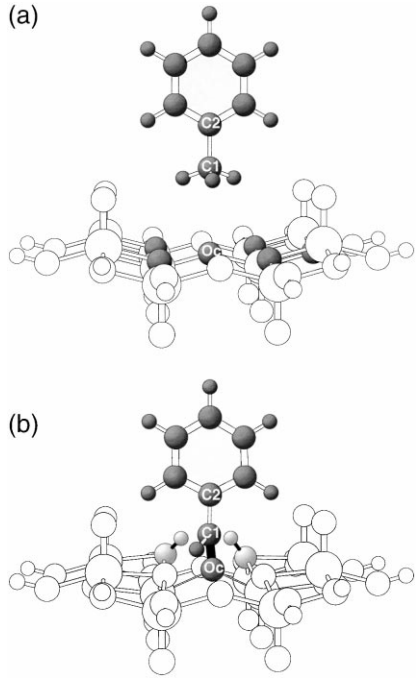

Fig. 6. Interaction of toluene with the $V_{10}O_{31}H_{12}$ cluster. The O, C and H atoms whose position are allowed to relax are denoted as shaded balls and labeled. Part (a) gives a starting geometry for the interaction (the organic molecule approaches the cluster in the direction perpendicular to the plane of the cluster, the CH_3-group pointing the bridging oxygen O(c). Part (b) shows a final product (precursor of an aldehyde). The C–O bond and two O–H surface hydroxyl groups (both between the H from the methyl group and triply coordinated O(d)) are shown in black.

6. Conclusions

The electronic binding in vanadium pentoxide is described by both ionic and covalent contributions. Structurally different surface oxygen atoms have different electronic and hence catalytic properties. Multicoordinated bridging oxygen atoms are characterized by an increased local reactivity with respect to electrophilic attacks as compared to singly coordinated vanadyl oxygen ions. The H/H^+ species which is split off as a result of the C–H activation near the V_2O_5(0 1 0) surface may stabilize at all surface oxygen sites forming stable hydroxyl groups. The

mechanism of this adsorption depends, however, on the structural and electronic properties of the adsorption site. The formation of the surface hydroxyls leads to significant weakening of respective V–O bonds with the weakened being strongest for V–O(c)–V bonds, i.e., for bonds between vanadium and doubly coordinated oxygen atoms. These oxygen sites become mobile in the presence of H/H^+ adparticles which indicates that they may be inserted into an organic molecule with highest probability. The calculations carried out for the interaction between hydrocarbons and the vanadium pentoxide surface substantiate this prediction. The interaction of propene and toluene with the $V_2O_5(0\ 1\ 0)$ surface starts with formation of a C=O bond between the carbon atom of the methyl group and the doubly coordinated oxygen and is followed by the abstraction of hydrogen from the methyl group. The C–H bond activation proceeds in both systems according to a similar mechanism which is, however, different from that on typical catalysts. Both parts of the broken C–H bond become attached to bridging surface oxide ions. The proton contributes to a surface OH-group, while the hydrocarbon fragment leads to an alkoxy group which, after loosing the second hydrogen, might desorb as an aldehyde leaving the oxygen vacancy behind.

References

[1] G. Ertl, H. Knötzinger, J. Weitkamp, see e.g. Handbook of Heterogeneous Catalysis, VCH/Wiley, Weinheim/New York, 1997.
[2] J. Tomasi, J. Mol. Struct. (Theochem.) 179 (1988) 273.
[3] B. Grzybowska-Swierkosz, J. Haber (Eds.), Vanadia Catalysts for Processes of Oxidation of Aromatic Hydrocarbons, PWN, Polish Scientific Publishers, Warsaw, 1984.
[4] A. Bielanski, J. Piwowarczyk, J. Pozniczek, J. Catal. 113 (1988) 334.
[5] M. Witko, K. Hermann, J. Mol. Catal. 81 (1993) 279.
[6] M. Witko, K. Hermann, in: S.V. Bellon, V.C. Corberan (Eds.), Stud. Surf. Sci. Catal. 82 (1994) 94.
[7] M. Witko, K. Hermann, R. Tokarz, J. Electr. Spectr. Rel. Phenomena 69 (1994) 89.
[8] K. Hermann, A. Michalak, M. Witko, Catal. Today 32 (1996) 321.
[9] A. Michalak, M. Witko, K. Hermann, Surf. Sci. 375 (1997) 385.
[10] M. Witko, R. Tokarz, J. Haber, J. Mol. Catal. 66 (1991) 205.
[11] M. Witko, R. Tokarz, J. Haber, J. Mol. Catal. 66 (1991) 357.
[12] M. Witko, Catal. Today 32 (1996) 89.
[13] M. Witko, R. Tokarz, J. Haber, J. Appl. Catal. A 157 (1997) 23.
[14] R.F. Nalewajski, J. Korchowiec, R. Tokarz, E. Broclawik, M. Witko, J. Mol. Catal. 77 (1992) 165.
[15] R.F. Nalewajski, J. Korchowiec, J. Mol. Catal. 82 (1993) 383.
[16] M.C. Zerner, G.H. Loew, R.F. Kirchner, U.T. Müller-Westerhoff, J. Am. Chem. Soc. 102, 589 (1980) 383.
[17] A.D. Bacon, M.C. Zerner, Theoret. Chim. Acta 53 (1979) 21.
[18] W.D. Edwards, M.C. Zerner, Theoret. Chim. Acta 72 (1987) 347.
[19] E. Wimmer, in: J.K. Labanowski, J.W. Andzelm (Eds.), Density Functional Methods in Chemistry, Springer, Heidelberg, 1991.
[20] A. Byström, K.A. Wilhelmi, O. Brotzen, Acta Chem. Scandinavica 4 (1950) 1119.
[21] H.G. Bachman, F.R. Ahmed, W.H. Barnes, Z. Kristallogr. Kristallgeom. Kristallphys. Kristallchem. 115 (1981) 110.
[22] R.W.G. Wyckoff, Crystal Structures, Interscience, Wiley, New York, 1965.
[23] The LCGTO–LSD–DFT program package DeMon was developed by A. St-Amant, D. Salahub at the University of Montral.
[24] N.U. Zhanpeisov, T. Bredow, K. Jug, Catal. Lett. 39 (1996) 111.
[25] G. Grymonprez, L. Fiermans, J. Vennik, Surf. Sci. 36 (1973) 370.
[26] M. Witko, R. Tokarz, K. Hermann, Polish J. Chem. 72 (1998) 1565.
[27] M. Witko, K. Hermann, R. Tokarz, A. Michalak, Proceedings of Symposium on Advances and Applications of Computational Chemical Modeling to Heterogeneous Catalysis, ACS Symposia, vol. 42, 1997, p. 94.
[28] G.W. Keulks, D. Krenzke, T.M. Notermann, Adv. Catal. 27 (1978) 183.
[29] R.K. Grasselli, S.D. Burrington, Adv. Catal. 30 (1981) 133.
[30] J. Haber, Proceedings of the Eighth International Congress on Catalysis, Berlin, 1984, Verlag Chemie-Dechema, Frankfurt, 1984, Plenary Lectures, vol. 1, p. 85.
[31] W.M.H. Sachtler, N.H. de Boer, Proceedings of the third International Congress on Catalysis, vol. 1, Amsterdam, 1964, North Holland, Amsterdam, 1965, p. 252.
[32] C.R. Adams, T.J. Jennings, J. Catal. 2 (1963) 63.
[33] C.R. Adams, T.J. Jennings, J. Catal. 3 (1964) 549.
[34] A.A. Davydov, IK Spektroskopija i Khimia Povierhnosti Okislov, Izd. Nauka, Novosibirsk, 1984.
[35] A.A. Davydov, V.G. Mikhaltchenko, V.D. Sokolovskii, G.K. Boreskov, J. Catal. 55 (1978) 299.
[36] R. Grabowski, J. Haber, J. Sloczynski, React. Kinet. Catal. Lett. 12 (1979) 119.
[37] B. Grzybowska-Swierkosz, J. Haber, J. Janas, J. Catal. 49 (1977) 150.
[38] J.D. Burrington, R.K. Grasselli, J. Catal. 59 (1979) 79.
[39] J. Haber, M. Witko, J. Mol. Catal. 9 (1980) 399.
[40] J. Haber, M. Sochacka-Witko, B. Grzybowska-Swierkosz, A. Golebiewski, J. Mol. Catal. 1 (1975/76) 35.
[41] J. Haber, M. Witko, A. Golebiewski, J. Mol. Catal. 3 (1977/78) 213.

[42] R. Gonzallez-Luque, M. Merchan, I. Nebot-Gil, F. Thomas, R. Montanna, J. Mol. Struct. (Theochem.) 120 (1985) 57.
[43] M. Merchan, I. Nebot-Gil, R. Gonzallez-Luque, F. Thomas, J. Mol. Struct. (Theochem.) 120 (1985) 479.
[44] M. Merchan, I. Nebot-Gil, R. Gonzallez-Luque, F. Thomas, Chem. Phys. Lett. 14 (1985) 516.
[45] V.D. Sokolovski, N.N. Bulgakov, React. Kinet. Catal. Lett. 6 (1977) 65.
[46] A.B. Anderson, D.W. Ewing, Y. Kim, R.K. Grasselli, J.D. Burrington, J.F. Brazdil, J. Catal. 6 (1985) 222.
[47] J. Haber, M. Witko, R. Tokarz, J. Mol. Catal., in print.
[48] A. Bielanski, J. Haber, Oxygen in Catalysis, Marcel Dekker, New York, 1990.
[49] P.J. Gellings, in: Special Periodical Reports, Catalysis, vol. 7, The Royal Society of Chemistry, London, 1985, p. 105.
[50] M. Witko, J. Haber, R. Tokarz, J. Mol. Catal. 82 (1993) 457.
[51] J. Haber, R. Tokarz, M. Witko, in: V.C. Corberan, S.V. Bellon (Eds.), Stud. Surf. Sci. Catal. 82 (1994) 739.